Development of Robust Video-oculography System for Non-invasive Autonomic Nerve Quantification

Masaru Kiyama, Hitoshi Iyatomi, and Koichi Ogawa
Department of Applied Informatics, Hosei University
Tokyo, Japan
Email: iyatomi@hosei.ac.jp

***Abstract*—There are many scientific literatures those have reported a relationship between autonomic nerves activity and neuropathy, such as depression, Alzheimer's disease. The quantification of autonomic nerves is expected to serve as a tool for quantifying the severity of the disease or for its early detection. Video-oculography is known as a non-invasive and reliable procedure of estimating autonomic nerves activity by a measurement of pupil response to a light stimulus. However, current video-oculography only performs a thresholding to detect the pupil area and therefore measuring the accurate transition of a pupil area is often difficult due to eyelid overlap, effects of blinking, eyelashes and so on. In this paper, we developed a video-oculography system consisting of a video-oculography scope with a newly-introduced stimulus controller and a robust pupil tracking algorithm. We evaluated the accuracy of our video-oculography system with respect to each impediment type and estimated typical pupillary light-reflex parameters, used in clinical practice. Our system achieved an extraction accuracy of 0.968 in the F-measure in average on a total of 9,714 tested image frames from 35 movies, and it showed much more robust over the most common impediment, the eyelid overlap, than other methods. In addition, we confirmed that our system could estimate pupillary light-reflex parameters appropriately.**

***Index Terms*—autonomic nerves, video-oculography, pupil reflex**

I. Introduction

Evaluation of activity of autonomic nerves is expected to serve as a tool for the quantification or early detection of depression or Alzheimer's disease [1]. Oculography or video-oculography is a non-invasive clinical method which monitors a pupil reflex of a patient responding to an impulse light stimulation [2] or involuntary movement of the pupil [3]. A pupil is controlled by two types of smooth muscles innervated by autonomic nerves, and the oculography evaluates the activity of these two opposite rolled nerves by monitoring a transition of pupil reflex.

Oculography has an advantage in inspection time compared with methods utilizing cardiac monitoring. However, currently-used video-oculography only performs a thresholding to split the pupil area from backgrounds and therefore, it cannot track accurate transition of the pupil size where the pupil area in an image frame is absent due to being covered by an eyelid (commonly seen) and especially affected by blinking, and has an over-estimation by eyelashes, etc.

Several researches on measuring the pupil reflex have been proposed [4]-[6]. Moriyama et al. [4] assumed pupil models and estimated a pupil area using a pattern matching strategy. This method is robust over noise and attains accurate estimation, but requires the construction of a patient-specific pattern and initial alignment. Sakashita et al. [5] estimated the pupil area by approximating an ellipse based on an inscribed parallelogram from tentatively extracted pupil area. This method is fast and interpolates abovementioned deficits or over-extraction, however it has a difficulty when the defect of the contour of the pupil exceeds around 30%.

In our previous study, we developed a robust pupil tracking algorithm for video-oculography [6] as the important first step for quantifying the autonomic nerve activities. This algorithm introduced an interpolation process which includes an active contour model, an ellipse estimation with a selection of reliable contour points, and a comparison process which considers the past frames addresses large deficits of the pupil area caused by blinking. It showed a superior performance in measuring pupil area from a captured image frame to conventional procedures. However, on the other hand, the evaluations have conducted only for cumulative of each image frame extracted from the movie and therefore (1) detailed investigations for robustness of the system over abovementioned impediments, and (2) evaluation of advanced result, i.e. pupillary light-reflex parameters [7], those are important findings for quantifying autonomic nerve activities in clinical practice, have not been made, yet.

In this paper, we made our video oculography system more practical. We newly embedded a signal controller to our video-oculography scope which permits us to control the timing and the duration of light stimulus for pupil area. An integrative investigation with the timing of light stimulus and the detected transition of the pupil size allows us to calculate pupillary light-reflex parameters. We performed two applicative evaluations and reported the results: (i) evaluation of robustness over impediments by category, such as the eyelid overlap including blinking and the eyelashes, and compared the performance with other methods (still evaluation), and (ii) evaluation of estimated pupillary light-reflex parameters under practical condition as a preliminary test (movie evaluation).

This research was partially supported by the Ministry of Education, Culture, Science and Technology of Japan (Grant-in-Aid for Young Scientists program (B), 23791295, 2011-2012).

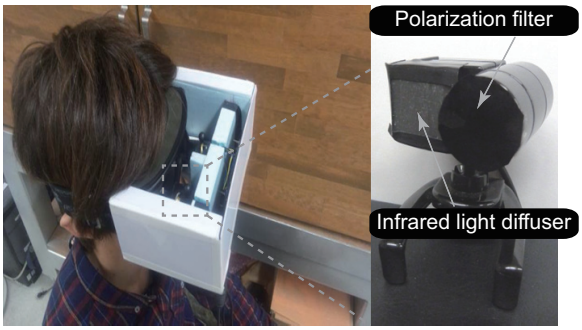

Fig. 1. Developed oculography scope

II. Measurement device and movies

A. Video-oculography system

Our pupil tracking system consists of the video-oculography scope and the processing algorithm. We built a video-oculography scope in accordance with the Pharmaceutical Affairs Act (Fig.1). The key components of our scope are an infrared camera, infrared LEDs for illumination, white LEDs for light stimulation on a pupil, a polarization filter for reducing spot noise in a video image, and an USB interface to a computer. A newly embedded signal controller with the scope allows us to control the timing and the duration of light stimulus.

The scope records a movie for a set amount of time including pupil reflex caused by a light stimulation. Our pupil area measurement algorithm on a USB connected computer determines the pupil area in each image frame. The transition of the pupil area is obtained by accumulating results from each image frame. We can estimate pupillary light-reflex parameters with the integrated analysis of the transition of determined pupil area and the timing of the light stimulus.

B. Movies

In this study, we used a total of 35 movies from 8 volunteer normal men captured by our new scope. The property of each movie has 640x480 pixels in resolution, 8-bit gray scale and the frame rate of 20. The duration of light stimulation for the pupil is 0.5 second (the same period is used in video-oculography in clinical practice) in each movie. Each movie includes at least one blink. The total number of calculated image frame was 9,714 in which the number of frames affected by eyelid and eyelash were 1,384 (14.2%) and 795 (8.2%), respectively. Note that all image frames were also affected by spot light noise caused by the infrared lighting.

We used additional 5 movies from one volunteer man (each of them consists of 290 frames) for evaluation of estimated pupillary light-reflex parameters.

III. Pupil tracking algorithm

We explain our pupil area measurement algorithm briefly here. Due to a limitation of the space, please refer our previous paper [6] in detail.

A. Pre-processing and initial extraction

An infrared illumination poses undesirable bright spots on a captured image. We introduced a polarization filter at the end of our infrared camera to reduce the abovementioned noise, and performed gamma correlation ($\gamma = 1.7$) to address darkened image by the filter. We performed a thresholding with the value θ to split a pupil area from the background. In our scope setting, we determined $\theta = 30$. Then, we set an ROI in the middle of an image and the largest region inside the ROI was regarded as the initial pupil area.

B. Determination of pupil area by selection of reliable contour points

An initially determined pupil area is often affected by the above-mentioned obstacles such as remaining bright spots, deficit by eyelid, blink, and effects by eyelashes or eyelash linear. In this phase, we estimated the appropriate pupil area with the following three steps. Fig.2 illustrates the scheme of this phase.

- step 1: We estimated the "contour candidates" of the pupil based on the initially determined pupil area using the active contour model [8] to reduce the false extraction mainly caused by eyelashes (Fig.2(a)).
- step 2: Select "reliable contour points" from their candidates obtained from the last step. This step is the main part of the overall pupil extraction algorithm. This step defines horizontal pairs of the candidate points (p_i, q_i) and calculates their centroid c_i for each pair (Fig.2(b)). Then we investigates the distribution of the centroids in vertical direction and if the large shift is detected between adjacent centroids (Fig.2(c)), we assume corresponding contour points are inadequate and eliminated from the candidates. Repeat this step until all points are stabilized.
- step 3: The pupil area is determined by means of an ellipse estimation using a least squares method with the reliable contour points. Ellipse parameters determined here are the position, major and minor axes of the pupil and its rotation (Fig.2(d)).

C. Verification of extraction with former frames

In most cases, pupil area in each image frame is adequately determined with the abovementioned phases. However, there are still some difficult cases where most of the pupil area is absent due to blinking etc. In order to address these cases, our algorithm examines the validity of the determined pupil area and perform re-extraction if necessary.

The algorithm compares the current detection result with former five image frames. If the deviation of the aspect ratio and the length of major axis of the estimated pupil are larger than the pre-defined threshold, the estimated pupil in the target frame is considered as inadequate. In this case, the center position of the pupil is determined referred to the method proposed by Kim et al. [9] and the pupil detection result of the adjacent frame (i.e. pupil size and shape) is inserted into the determined center.

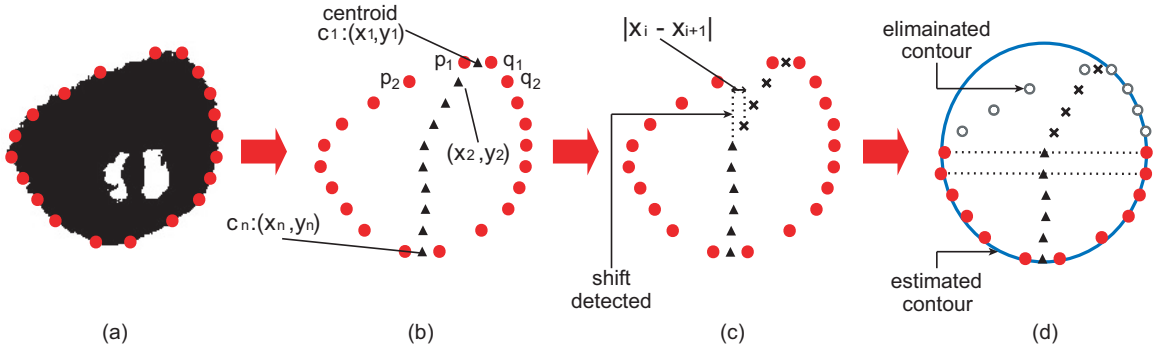

Fig. 2. Determination of pupil area by selection of reliable contour points

IV. Experiment

A. Evaluation of pupil area detection over obstacles

In order to perform a quantitative evaluation, we manually specified the pupil area for all image frames and used them as the gold standard. As the evaluation criteria, we used *precision* and *recall* in our studies. In general terms, precision is a measure of the accuracy of the extraction and recall is a measure of how much of the pupil is covered by the extraction. Since precision and recall are trade-off criteria, we also used F-*measure* criterion ($= 2\times$ precision $\times$ recall / (precision + recall)) to evaluate general extraction performance. Note that the range of F-measure is [0,1] and the larger score indicates the better performance. We compared the performance with Sakashita's method [5] and the method with a simple thresholding method (equivalent to conventional video-oculography) as a reference.

B. Estimation of pupillary light-reflex parameters

We estimated pupillary light-reflex parameters [7] using our video-oculography score as a preliminary examination. The subject was given 90 seconds for scotopic adaptation before starting the test and each light stimulation was given with 60 seconds interval. Within pupillary light-reflex parameters, we selected intelligible four parameters such as $CR, T1, T3$ and $T5$ as shown in Fig.3. We compared the estimated parameters between those from our algorithm and the gold standard (pupil area in each image frame was determined manually).

V. Experimental Results

Fig.4 shows typical examples of pupil detection in which pupil areas are affected by some issues, (a) and (b): eyelashes, (c) and (d): eyelid and blink. The detection performance of the pupil area categorized by impediment type was summarized in Tables I and II. In these tables, bold figure indicates the best in each category. Our algorithm achieved a precision of 96.9%, recall of 96.8%, and F-measure of 0.968 in average and kept high detection accuracy under non-ideal conditions. In all noise categories, the proposed algorithm showed superior performance to other methods. Especially for image frames affected by eyelid, proposed algorithm attained much better performance than others.

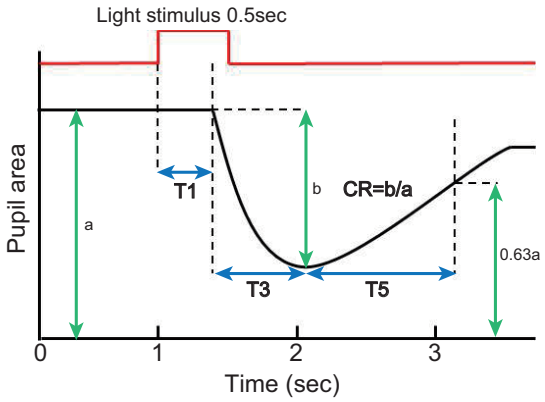

Fig. 3. Four pupillary light-reflex parameters in this study

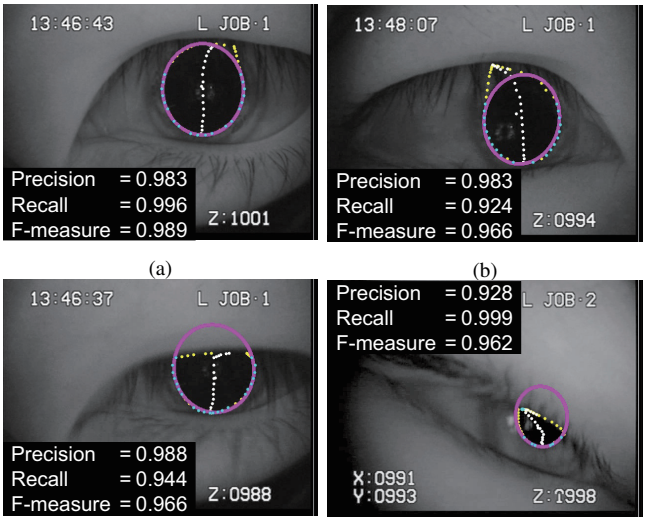

Fig. 4. Examples of pupil area detection

Fig.5 shows an example of the obtained transitions of pupil size. Table III shows the estimated pupillary light-reflex parameters. In each parameter, estimated parameter (est.), gold standard (target) and estimation error (err (%)) are listed. The average processing time was 0.09 sec/frame using Panasonic Let's Note S9 notebook PC (Intel Core i5-520M processor, 4GB memory).

TABLE I
COMPARISON OF PUPIL AREA DETECTION PERFORMANCE IN F-MEASURE

Method / noise category	eyelid	eyelash	others
Proposed method	**0.951**	**0.964**	**0.971**
overall: F, (precision, recall)	**0.968, (96.9%, 96.8%)**		
Sakashita's method [5]	0.890	0.938	0.967
overall: F, (precision, recall)	0.954, (96.5%,94.8%)		
Simple thresholding method	0.875	0.932	0.938
overall: F, (precision, recall)	0.926, (97.9%, 88.2%)		

TABLE II
STATISTICS OF PUPIL DETECTION ACCURACY

Condition / category	F-measure† / method	95+ (%)	90+ (%)	85+ (%)	80+ (%)
eyelid	Proposed	**69.29**	**91.91**	**95.66**	**98.41**
	Sakashita [5]	34.32	59.61	75.79	85.33
	thresholding	9.61	54.55	73.55	85.04
eyelash	Proposed	**87.80**	**96.10**	**98.62**	**98.74**
	Sakashita [5]	57.61	94.21	96.10	96.48
	thresholding	44.14	95.72	96.85	97.11
others	Proposed	89.11	**97.80**	**99.00**	**99.32**
	Sakashita [5]	**89.86**	97.53	98.30	98.74
	thresholding	47.67	87.11	95.41	98.26
overall	Proposed	**85.84**	**96.44**	**98.11**	**98.76**
	Sakashita [5]	76.94	89.11	92.07	93.75
	thresholding	41.48	82.22	91.35	95.18

Bold figure indicates the best in each category.
†: Cumulative percentages of the number of image frames exceed the F-measure.

VI. DISCUSSION

Our pupil area detection algorithm was designed to overcome shortcomings of conventional video-oculography. From Tables I and II, we confirmed that our algorithm was robust over impediments, especially for eyelid overlap. From the distribution of F-measures, 91.9% of image frames overlapped by the eyelid exceeded the F-measure of 90 with our method, while Sakashita's method was around 60% and the simple thresholding method used in conventional video-oculography was 55%. This advantage was mainly owing to the specially designed interpolation process described in section III.B (especially its step2). Eyelid overlap was commonly seen in practical (14.2% of image frames in this test). The robustness for this was a crucial feature for a practical video-oculography.

From Table III (parameter evaluation), average of absolute error in estimating pupillary parameter for $T1, T3$ and $T5$ were 0.01-0.06 seconds (= 4.0-6.2% in parametrical error). Relatively large error ratio for pupillary parameters compared with the absolute measurement error was mainly due to the limitation of time resolution caused by hardware (20fps) in this test (see $T1$ for example - error of 0.05 sec was equivalent to parametrical error of 20%). We expect that this will be reversible with introducing a faster camera device.

VII. CONCLUSION

We concluded that our video-oculography system tracked pupil area accurately even in non-ideal conditions and showed a strong capability to estimate pupillary light-reflex parameters. We consider that our system with adequate improvements will be of help in quantification or early detection of depression, Alzheimer's diseases etc. in near future.

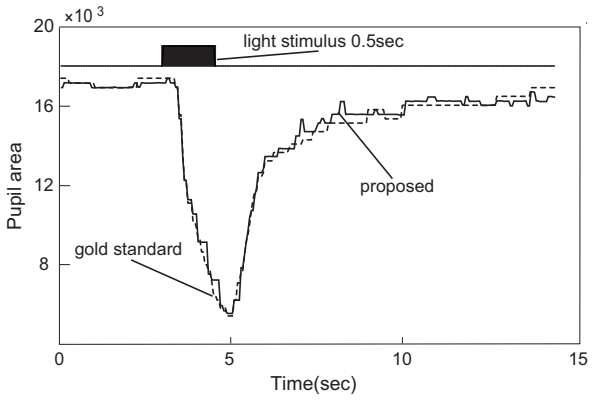

Fig. 5. Transition of the pupil area with a light stimulus

TABLE III
ESTIMATED PUPILLARY LIGHT-REFLEX PARAMETERS

parameter		1st.	2nd.	3rd.	4th.	5th.	E[err]†
CR (%)	est.	60.25	64.06	67.34	70.70	68.78	
	target	62.48	66.84	68.96	70.76	69.50	1.48%
	err(%)	-3.56	-4.16	-2.36	-0.09	-1.03	2.32%
T1 (sec)	est.	0.20	0.35	0.45	0.25	0.60	
	target	0.25	0.35	0.45	0.25	0.60	0.01 sec
	err(%)	-20.0	0.00	0.00	0.00	0.00	4.00%
T3 (sec)	est.	0.60	1.00	1.45	0.65	1.10	
	target	0.65	1.00	1.45	0.55	1.10	0.03 sec
	err(%)	-7.69	0.00	0.00	18.18	0.00	5.17%
T5 (sec)	est.	1.30	1.15	1.00	0.70	1.15	
	target	1.30	1.20	1.05	0.85	1.10	0.06 sec
	err(%)	0.00	-4.17	-4.76	-17.65	4.55	6.22%

†:Average of absolute error.

REFERENCES

[1] S.Elmstahl, M.Petersson, B.Lija, S-M.Samuelssob, I.Rosen, and L.Bjuno, "Autonomic Cardiovascular Responsesto Tilting in Patients with Alzheimer's Disease and in Healthy Elderly Women", Age Ageing Vol.21, No.4, pp301-307, 1992.

[2] K.Fountoulaki, F.Fotiou, A.Iacovides, J.Tsiptsios, A.Goulas et al., "Changes in pupil reaction to light in melancholic patients," International Journal of Psychophysiology, Vol.31, No.2, pp.121-128, 1999.

[3] R.E.Gans, "Video-oculography: A new diagnostic technology for vestibular patients," The Hearing Journal, Vol.54, No.5, pp.40-42, May 2001.

[4] T.Moriyama, T.Kanade, T.J.Xiao, and J.F.Cohn, "Meticulously Detailed Eye Region Model and Its Application to Analysis of Facial Images," IEEE Trans. on Pattern Analysis and Machine Intelligence ,Vol.28, No.5, pp.738-752, 2006.

[5] Y.Sakashita, H.Fujiyoshi, Y.Hirata, H. Takamaru, and N.Fukaya, "Real-Time Measurement of Cycloduction Movement Based on Fast Ellipse Detection," Electronics and Communications in Japan, Vol.92, No.11, pp.9-18, 2009.

[6] M.Kiyama, H.Iyatomi, and K.Ogawa, "Robust Video-Oculography for Non-Invasive Autonomic Nerve Quantification," Proc. IEEE EMBC 2011, pp.494-497, 2011.

[7] A.Wakasugi and T.Hanawa, "Establishing an objective method for assessment the effects of Kampo medicine," Journal of Traditional Medicines, Vol.25, pp.1-5, 2008.

[8] M. Kass, A.Witkin, and D.Terzopoulos,"Snakes Active contour models," International Journal of Computer Vision, Vol.1, No.4, pp.321-331, 1988.

[9] S.C.Kim, K.C.Nam, W.S.Lee, and D.W.Kim, "A new method for accurate and fast measurement of 3D eye movements," Medical Engineering & Physics Vol.28, pp.82-89, 2006.